PSO Optimized PID Regulator for a Variable Frequency Brushless Synchronous Generator

Hassen SMAIL[1], *Mostafa Kamel SMAIL*[2], *Cherif FETHA*[1], *Tahar BAHI*[3]

[1]Electrical Engineering Departement, Faculty of Technology, University of Batna 2,
Route de Constantine 53, Fesdis, 05078 Batna, Algeria
[2]Institut Polytechnique des Sciences Avancees (IPSA), Boulevard de Brandebourg 63,
94200 Ivry-sur-Seine, France
[3]Electrical Engineering Departement, Faculty of Engineering Sciences,
Badji Mokhtar - Annaba University, BP 12, 23000 Annaba, Algeria

h.smail@univ-batna2.dz, mostafa-kamel.smail@ipsa.fr, cheriffetha@gmail.com, tbahi@hotmail.fr

DOI: 10.15598/aeee.v16i4.2344

Abstract. *The aim of this paper is to describe development of a new control structure for Automatic Voltage Regulator system. This approach is based on the optimization of the control voltage magnitude of a brushless excitation synchronous alternator machine operating at variable speed. The choice of the machine type is justified by its attractiveness in several areas such as the aircraft domain due to its autonomy and robustness. The considered control technique is based on the simultaneous optimization of two regulators introduced in the loop control. The parameters of the Proportional Integral Derivatives (PID) regulator have been optimized using the Particle Swarm Optimization (PSO), which is considered as an attractive method considering the wide operating speed range, and the load variations compared with the classical methods such as Ziegler Nichols. Many robustness tests are carried out by considering the parameters variations as well as the perturbation connection and disconnection of the load at low and high speeds.*

Keywords

Optimization, PID, PSO, Synchronous Generator with Brushless Exciter, variable speed, voltage amplitude control.

1. Introduction

The production of the electrical energy with variable speed alternators seems to be the best solution in terms of performance and reliability [1]. This system is based on a combination of a generator that operates at variable speed and a training motor. A static converter is associate at the output of the generator in order to stabilize the suitable frequency [2].

The choice of a variable frequency generation is based on the machine type and field of application that allows the reduction of the mechanical losses, the gearbox costs and the size of the assembly.

The production of embedded electrical energy is characterized by a wide training speed of the alternator that is used in several applications including aircraft field [3]. However, the wide training speed introduces constraints in voltages and currents in the load. In this regard, several studies have been published and allowed choosing the alternator and its suitable control strategy [4] and [5].

The advances in power electronics allow us a new challenge in the area of electrical production. From a mechanical source of variable speed, a fixed frequency and a regulated constant voltage can be obtained via a static converter. Which has the advantages of reducing the generator size and weight, since the mechanical regulation system of speed is removed, as in the new aircraft supply system [4].

The variable speed operation allows an optimization in the energy captured by a turbine, but it requires the implementation of a converter and its control. Which leads to an additional cost in comparison to a fixed speed operation [4] and [6].

In case of hybrid vehicles, all the studies conducted on the variable speed generators have shown that diesel consumption is optimized and reduced comparatively to their operating at a fixed speed [5], [6] and [7].

A wide range of speed variation, in driving the Brushless Excitation Synchronous Generator (BESG) engine, penalizes the stability of the output voltage control of the main generator. To remedy this, several studies have been initiated to improve and develop new control techniques [8].

The schematic mechanism of BESG is illustrated in Fig. 1. The generator is assumed equivalent to three separated machines placed in cascade, such as Permanent Magnet Generator (PMG), synchronous machine and alternator. The PMG machine allows the generator a completely autonomous operation. The supply voltage for this machine is adjusted to feed a connected chopper to the second synchronous machine. The three-phases are powered through a converter. The mono-phase inductor is placed in the stator side while the three-phase armature is placed in the rotor.

The obtained voltages are used to feed the inductor of the main generator, and these voltages are adjusted from the rotor through six rotating diodes. This configuration is a conventional synchronous machine with a conventional wound inductor connected to the network or load. It's noticed for this configuration, the absence of brushes which causes the increase the cost and the real complexity of the generator. The frequency of the obtained voltages is in function of the rotation speed [9].

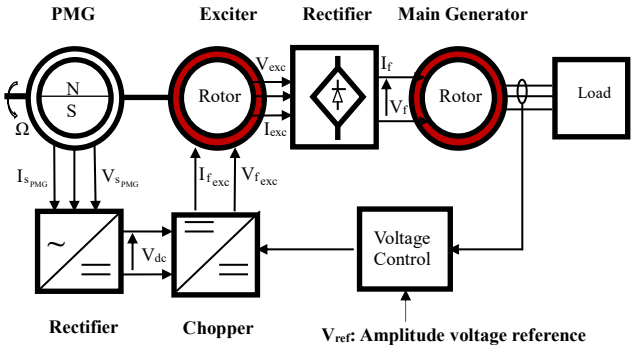

Fig. 1: Schematic mechanism of brushless excitation synchronous generator.

In the literature, the control for the main generator voltage regulation is based on three actions. The first one is the inner feedback loop that controls the excitation current of the exciter. The second action is the outer feedback loop for direct output voltage regulation of the main generator. And the third one is the disturbance-rejection loop that compensates the changes in the output voltages caused by the generator load (i.e., stator) current. The global loop is introduced for the voltage control of the machine [8].

This technique offers stability to the total voltage of the alternator and rejects all disturbances regardless of the variation of the rotation speed or load. But the proposed control technique is very difficult to be implemented in practice, due to the complexity of the block diagram and they depend on the machine parameters that affect the stability of the system.

In order to stabilize and simplify the control, a new technique is developed in the present work. This technique consists of calculating the voltage excitation of the principal exciter-generator that corresponds to the nominal voltage output of the main generator. The voltage excitation is inversely proportional to the rotation speed.

This excitation is the reference of the regulator of the machine with permanent magnets. Thus, the proposed control technique comprises two Proportional-Integral-Derivative (PID) controllers; the first one for the regulation of the output voltage of the PMG and the second one for the regulation of the main generator terminal voltage. In order to optimize the PID controller parameters, the Particle Swarm Optimization (PSO) has been used.

The PID control is the most efficient and widely used feedback control strategy, due to its simplicity and satisfactory control performance. The wide use of PID control has sustained research on finding the key methodology for PID tuning to obtain the best possible performance out of the PID control. Optimal control performance can only be achieved after identifying the finest set of Proportional gain (K_p), Integral gain (K_i) and Derivative gain (K_d).

Artificial intelligence methods, such as neural network, fuzzy system, and neural-fuzzy logic have been widely applied to optimize the PID controller parameters. Many iterative techniques, such as Genetic Algorithm (GA), Simulated Annealing (SA) and Chaotic Algorithm (CA) have recently received much attention for achieving high efficiency and searching global optimal solution in problem space [10], [11] and [12].

Particle Swarm Optimization (PSO) as one of the modern heuristic algorithms, was developed through simulation of a simplified social system and has been found to be robust in solving continuous nonlinear optimization problems. The PSO technique can generate a high-quality solution within shorter calculation time and stable convergence characteristic than other stochastic methods [11].

The adopted control technique is composed of two loops and two regulators. The first loop is for the output voltage of PMG controller, induce an overvoltage protection of the system, while the second loop is for the total voltage regulation. Therefore, it is found to be simple compared to the three-loop technique and the system rejected all disturbances (Fig. 1).

Since the machine works in a wide speed range, finding the regulator parameters (K_p, K_i and K_d) values is very difficult. Moreover, the determination of these parameters by direct conventional methods like Ziegler Nichols (ZN) and Internal Model Control (IMC) is somewhat complicated. Therefore, the Particle Swarm Optimization (PSO) method is used to find optimal values of these parameters. PSO is an iterative optimization method that can handle complex systems that are composed of several blocks.

In our application, the PSO tends to minimize both response times, overshoot and difference between the reference voltage and the actual final voltage of the main generator [13].

The advantage of using two regulators is the limitation of the voltage generated by PMG which produced at high speed. This protection allows the system to operate in a wide range of speed [14].

In this paper, a machine drive is considered as a speed source, i.e. the alternator output is low compared to mechanical power drive: a case of the energy production embedded [4].

This paper is organized as follows. Firstly, the presentation and modulization of BEGS will be presented in Sec. 2. Then the formulation of the optimization technique will be treated in Sec. 3. Finally, the simulation results and robustness study will be presented in the last section in order to illustrate the efficiency of the proposed control technique.

2. Presentation of BESG

The synchronous BESG machine, or nominated the Variable Frequency Generator, is shown in Fig. 1. It is composed of three separate synchronous generators linked in cascade, from the left to right. The first machine contains a PMG, which allows the BESG to be fully autonomous in terms of excitation. The second machine is an inverse synchronous machine structure (or exciter). The output voltage of the PMG will supply the Chopper after rectification. The output voltage of the chopper will regulate the second stage of the BESG. The output of the second stage that comes from the armature (rotor) will be rectified, by a diode bridge rectifier, to supply the inductor main generator, which represents the last stage. And at the end, the output of the main generator will supply the load.

The main feature of the synchronous BESG machine is the absence of the mechanical friction which increases the cost and the complexity of the generator.

The output voltage frequency of the BESG machine is related to the common rotational speed of the three machines. The adopted BESG machine structure can be found in several applications, where the power could be produced in a variable speed drive, for example in some industrial applications, energy production, embedded or renewable energy [15].

2.1. Modelling and Block Diagram of the Main Generator

In practice, the machines are known by their windings and their designs. In order to analyse and take into account their exact configurations, we shall develop, for each type of machine, a model that can be close to the real model to be rigorously controlled. The BESG machine consists of three synchronous machines (PMG, inverse synchronous machine and main generator) whose models are very similar to the PMG with slight differences. In order to modelize the main generator, the Park Transformation is used to write the synchronous machine model. In our application, the rotation speed and the voltage excitation will be the input of the model. The output of the main generator model is voltage. By neglecting the effects of shocks, regarding the small values of the time constants, the model will be described by the following equations:

Voltage equations:

$$\begin{cases} v_d = R_s i_d + \frac{\mathrm{d}\Phi_d}{\mathrm{d}t} - \omega\phi_q, \\ v_q = R_s i_q + \frac{\mathrm{d}\Phi_q}{\mathrm{d}t} - \omega\phi_d, \\ v_f = R_f i_f + \frac{\mathrm{d}\Phi_f}{\mathrm{d}t}, \end{cases} \tag{1}$$

where v_d, v_q, i_d and i_q are voltages and currents in dq frame (direct and transverse axe); v_f and i_f are voltage and current of the main field winding; R_s is stator resistance; R_f is main field resistance, Φ_d, Φ_q are flux in dq frame, ω is the electrical angular speed of the BESG. The mechanical speed is supposed variable, it's very important in our proposed control strategy.

Flux equations:

$$\begin{cases} \phi_d = L_d i_d + M_{fd} i_f, \\ \phi_q = L_q i_q, \\ \phi_f = L_f i_f + M_{fd} i_d, \end{cases} \tag{2}$$

where L_d and L_q are the direct and transverse stator main inductances; L_f is the main field inductance. M_{fd} is the mutual inductance between direct stator winding and main field.

Substituting the flux Eq. (2) into the voltages Eq. (1) leads to write the model of the stator voltage (induced) in the matrix form as follows:

$$[V_s] = [Z_s] \cdot [I_s] + M_{fd} \cdot \omega \cdot \begin{bmatrix} 0 \\ 1 \end{bmatrix} i_f. \tag{3}$$

With

$$[V_s] = \begin{bmatrix} v_d & v_q \end{bmatrix}^t, [I_s] = \begin{bmatrix} i_d & i_q \end{bmatrix}^t, \tag{4}$$

$$[Z_s] = \begin{bmatrix} R_s + S \cdot L_d & -\omega \cdot L_q \\ \omega \cdot L_d & R_s + S \cdot L_q \end{bmatrix}, \quad (5)$$

where S is the Laplace operator ($S = \mathrm{d}/\mathrm{d}t$), V_s, I_s and Z_s are the Voltage, Current and the Impedance of the main generator, respectively.

The substitution of the flux Eq. (3) in voltages Eq. (1), of the inductor, allows deducing the following operating equations:

$$i_f = \frac{1}{R_f + S \cdot L_f} U_f, \quad (6)$$

with

$$v_f = i_f(R_f + S \cdot L_f) + S \cdot M_{fd} \cdot i_d, \quad (7)$$

where

$$U_f = i_f(R_f + S \cdot L_f), e_{fd} = S \cdot M_{fd} \cdot i_d. \quad (8)$$

Thus

$$v_f = U_f + e_{fd}, \quad (9)$$

where e_{fd} is the compensation factor.

A linear control of the synchronous machine excitation circuit, which corresponds to the current, if with the voltage v_f, requires the compensation of the transfer e_{fd} that represents the EMF (null continuous).

Introducing Eq. (6) into equation Eq. (4) leads to writing the model of the synchronous machine for an alternator by inversing the sign of the stator voltage on the load level, as follows:

$$[V_s] = [Z_s] \cdot [I_s] + \frac{M_{fd} \cdot \omega}{R_f + S \cdot L_f} \cdot \begin{bmatrix} 0 \\ 1 \end{bmatrix} \cdot (v_f - e_{fd}). \quad (10)$$

The matrix Eq. (10) can be formulated as follows:

$$[V_s] = [Z_s] \cdot [I_S] + \begin{bmatrix} 0 \\ 1 \end{bmatrix} \cdot \left(\frac{M_{fd}}{R_f + S \cdot L_f} v_f - \frac{S \cdot M_{fd}^2}{R_f + S \cdot L_f} i_d \right). \quad (11)$$

If the alternator is required to debit on the load, in 2D park components, the direct and quadrature components of the load voltage are given by:

$$\begin{cases} -v_d = R_l \cdot i_d + L_l \frac{di_d}{dt} - \omega \cdot L_l i_q, \\ -v_q = R_l \cdot i_q + L_l \frac{di_q}{dt} - \omega \cdot L_l i_d. \end{cases} \quad (12)$$

Equation (11) can be expressed by:

$$[-V_s] = [Z_l] \cdot [I_l], \quad (13)$$

with

$$[Z_l] = \begin{bmatrix} R_l + S \cdot L_l & -\omega \cdot L_l \\ \omega \cdot L_l & R_l + S \cdot L_l \end{bmatrix}, \quad (14)$$

where R_l, L_l and Z_l are the resistance, the inductance and the impedance of the load connected to the main generator.

With the matrix Eq. (10) and Eq. (11), the block diagram of the generator supplying a load is illustrated in Fig. 2.

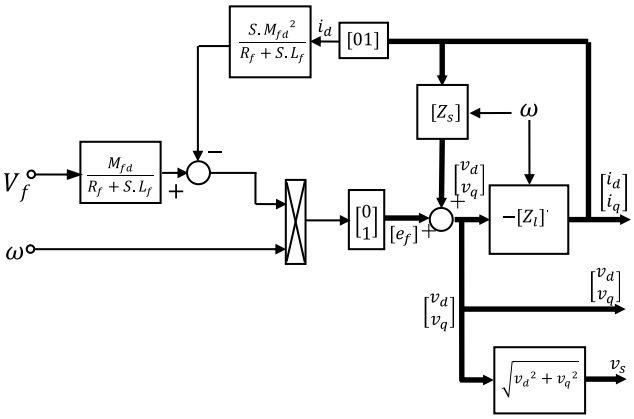

Fig. 2: Block of a main generator supplying an inductive load.

2.2. Modelling and Functional Diagram of the Exciter and Rectifier

The exciter represents the excitation system that supplies the inductor of the main generator. The exciter is a three-phase synchronous machine with fixed excitation (stator) and without damper whose phases are carried by the rotor with a six-diode bridge connected to its terminals. The six diodes are mounted on the rotor in order to feed the inductor of the main generator with DC (Fig. 1).

The exciter circuit is modelled by the same approach as used for the main generator. The excitation voltage of the exciter system will be considered as the power source for the excitation of the main generator through a rectifier diode (Fig. 1).

For the exciter model, the same equations of the main generator model will be used, where all the variables will be written from the rotor side of the exciter, as shown in Fig. 3.

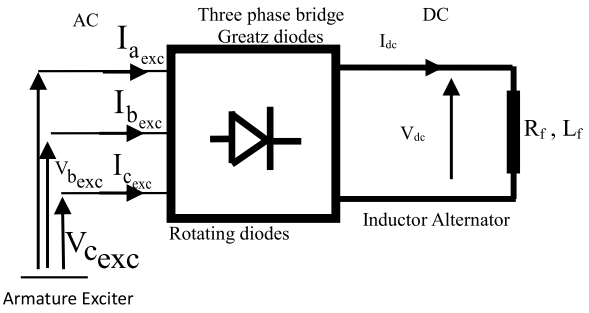

Fig. 3: AC to DC conversion using rotating diode bridge.

The effective rectified voltage is given by:

$$V_{aff_{exc}} = \frac{\sqrt{v_{d_{exc}}^2 + v_{d_{exc}}^2}}{\sqrt{2}}. \quad (15)$$

The average value of the output voltage of a rectifier for q phase's number is:

$$V_{dc} = \frac{2q}{\pi}\sin\left(\frac{\pi}{q}\right)\cdot V_{aff_{exc}}. \tag{16}$$

To calculate the new values of the load exciter after recovery, an equality of powers between the input and the output of the converter is considered as follows:

$$P_{AC} = 3V_{aff_{exc}}\cdot I_{aff_{exc}}\cdot\cos(\varphi_{exc}) = V_{dc}\cdot I_{dc} = P_{dc}. \tag{17}$$

Thus, the alternating side can be observed, which is seen continuous, in terms of active power, if the losses in the diodes are neglected:

$$P_{AC} = \frac{3V_{eff_{exc}}^2}{R_{l_{exc}}} = \frac{V_{dc}^2}{R_f} = P_{dc}. \tag{18}$$

From the knowledge of power electronics, the DC voltage (average rectified) for q number phases can be written:

$$V_{dc} = \frac{2q}{\pi}\sin\left(\frac{\pi}{q}\right)\cdot V_{eff_{exc}}. \tag{19}$$

For the three-phase case:

$$q = 3 \rightarrow V_{dc} = \frac{3\sqrt{3}}{\pi}V_{eff_{exc}}. \tag{20}$$

DC restated for q phases:

$$I_{dc} = \sqrt{\frac{q}{2}}I_{eff_{exc}}. \tag{21}$$

For the three-phase case:

$$q = 3 \rightarrow I_{dc} = \sqrt{\frac{3}{2}}I_{eff_{exc}}. \tag{22}$$

Powers equality AC & DC allows writing:

$$P_{AC} = P_{dc}. \tag{23}$$

In terms of active power, if the losses in the diodes are neglect:

$$R_{l_{exc}} = \frac{\pi^2}{9}R_f. \tag{24}$$

This gives, after calculating AC side:

$$\begin{aligned} L_{l_{exc}}\cdot\omega = R_{l_{exc}}\cdot\tan(\varphi_{exc}) = \\ = R_{l_{exc}}\sqrt{\frac{1}{\cos^2(\varphi_{exc})}-1}. \end{aligned} \tag{25}$$

The value of $\tan\varphi$ obtained by Eq. (24) is replaced in Eq. (16), the expression of $L_{l_{exc}}$ is obtained by:

$$\begin{aligned} L_{l_{exc}} = \frac{1}{\omega}R_{l_{exc}}\cdot\tan(\varphi_{exc}) = \\ = \frac{1}{3\omega}R_{l_{exc}}\sqrt{2\pi^2-9}. \end{aligned} \tag{26}$$

Thus, $L_{l_{exc}}$ is relatively low.

Equation (24) and Eq. (25) are integrated into the overall simulation model, which is very close to the real system.

2.3. Modelling and Functional Diagram of PMG

The PMG provides the power to the control system of the excitation of the exciter. The application of Park Transformation to the PMG model corresponds to transform the three coils (stator) two equivalent coils. With the same approach used for the main generator, we assume that the rotor of the PMG machine is flat, and the magnetic circuit is not saturated. The equations are defined as follow:

$$[V_{s_{pmg}}] = [Z_{s_{pmg}}]\cdot[I_{s_{pmg}}] + \phi_{pmg}\cdot\omega\cdot\begin{bmatrix}0\\1\end{bmatrix}. \tag{27}$$

With:

$$[V_{s_{pmg}}] = [V_{d_{pmg}} \quad V_{q_{pmg}}]^t. \tag{28}$$

$$[I_{s_{pmg}}] = [I_{d_{pmg}} \quad I_{q_{pmg}}]^t. \tag{29}$$

$$[Z_{s_{pmg}}] = \begin{bmatrix} R_{s_{pmg}} + S\cdot L_{d_{pmg}} & -\omega\cdot L_{q_{pmg}} \\ \omega\cdot L_{d_{pmg}} & R_{s_{pmg}} + S\cdot L_{q_{pmg}}\end{bmatrix}. \tag{30}$$

The symbols of the last equations are the same as those described previously. The mechanical speed of the PMG machine is considered variable.

When the PMG is loaded, the direct and quadrature components of the voltages are given by:

$$\begin{cases} -v_{d_{pmg}} = R_{l_{pmg}}\cdot i_{d_{pmg}} + L_{l_{pmg}}\dfrac{\mathrm{d}i_{d_{pmg}}}{\mathrm{d}t} - \\ \qquad \omega\cdot L_{l_{pmg}}\cdot i_{q_{pmg}}, \\ -v_{q_{pmg}} = R_{l_{pmg}}\cdot i_{q_{pmg}} + L_{l_{pmg}}\dfrac{\mathrm{d}i_{q_{pmg}}}{\mathrm{d}t} - \\ \qquad \omega\cdot L_{l_{pmg}}\cdot i_{d_{pmg}}. \end{cases} \tag{31}$$

Equation (27) and Eq. (31) in matrix and operational form are written as:

$$[-V_{s_{pmg}}] = [Z_{l_{pmg}}]\cdot[I_{s_{pmg}}]. \tag{32}$$

With:

$$[Z_{l_{pmg}}] = \begin{bmatrix} R_{l_{pmg}} + S\cdot L_{l_{pmg}} & -\omega\cdot L_{l_{pmg}} \\ \omega\cdot L_{l_{pmg}} & R_{l_{pmg}} + S\cdot L_{l_{pmg}}\end{bmatrix}. \tag{33}$$

With the matrix Eq. (27) and Eq. (32), the block diagram of a generator supplying a load is illustrated by Fig. 4.

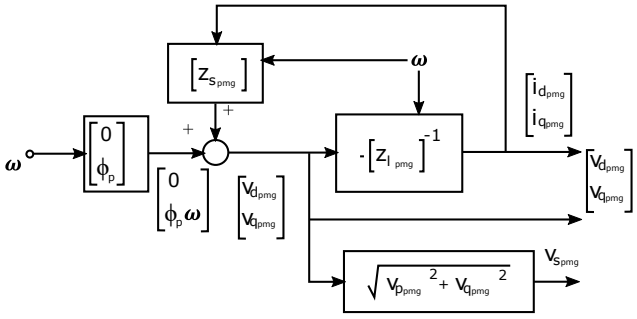

Fig. 4: Block diagram of permanent magnet alternator supply the inductive load.

2.4. Formulation of the Optimization Problem

In this problem, the reference voltage, the response time, and the overshoot are regulated by optimizing the PID controller parameters. PSO is used to minimize the objective function F given in [15], where O_{sh} is the maximum overshoot of change in terminal voltage, t_{st} is the settling time of change in terminal voltage (s) and max_dv is the maximum derivative of charge in terminal voltage.

$$F = (O_{sh} \cdot 1000) + t_{st}^2 + \frac{0.001}{\max\_dv^2}. \tag{34}$$

3. Particle Swarm Optimization

The PSO is an evolutionary algorithm for the solution of optimization problems. It belongs to the field of Swarm Intelligence and Collective Intelligence and is a sub-field of Computational Intelligence [16]. It was developed by Eberhart and Kennedy and inspired by social behaviour of bird flocking or fish schooling [17]. The PSO method is regarded as a population-based method, where the population is referred to as a swarm [18]. The swarm consists of n individuals called particles, each of which represents a candidate solution [19]. Each particle i in the swarm holds the following information:

- it occupies the position x_i,
- it moves with a velocity v_i,
- the best position, the one associated with the best fitness value particle has achieved so far pbesti,
- the global best position, the one associated with the best fitness value found among all of the particles *gbest*.

In our application, the positions of particles x_i represent the parameters of PID controller (K_d, K_i and K_p).

$$G(S) = K_p + \frac{K_i}{S} + S \cdot K_d. \tag{35}$$

$G(S)$ is the transfer function of the PID controller. The fitness of a particle is determined from its position. The fitness is defined in such a way that a particle closer to the solution has higher fitness value than a particle that is far away. In each iteration, velocities and positions of all particles are updated to persuade them to achieve better fitness according to the following equations:

$$\begin{aligned} v_{ij}^{t+1} = v_{ij}^t + c_1 \cdot rand_{1j}^t \cdot (pbest_{ij}^t - x_{ij}^t) \\ +c_2 \cdot rand_{2j}^t \cdot (pbest_{ij}^t + x_{ij}^t), \end{aligned} \tag{36}$$

$$x_{ij}^{t+1} = x_{ij}^t + v_{ij}^{t+1}, \tag{37}$$

for $j = 1, ..., d$ where d is the number of dimensions, $i = 1, ..., n$ where n is the number of particles, t is the iteration number, w is the inertia weight, $rand1$ and $rand2$ are two random numbers uniformly distributed in the range [0,1], c_1 and c_2 the acceleration factors.

The c_1 is the cognitive acceleration constant. This component propels the particle towards the position where it had the highest fitness. The c_2 is the social acceleration constant. This component steers the particle towards the particle that currently has the highest fitness.

The inertia weight w affects the contribution of v_{ij}^t to the new velocity $v_{ij}^{(t+1)}$. If w is large, it makes a large step in one iteration (exploring the search space), while if w is small, it makes a small step in one iteration, therefore tending to stay in a local region [20].

Typically, the velocity of a particle is bounded between properly chosen limits $v_{\min} < v_{id} < v_{\max}$ (in most cases $v_{\min} = -v_{\max}$). Likewise, the position of a particle is bounded as follows: $x_{\min} < x_{id} < x_{\max}$.

Afterwards, each particle updates its personal best position using the following equation:

$$pbest_i^{t+1} = \begin{cases} pbest_i^t, & \text{if } f(pbest_i^t) < f(x_i^{t+1}), \\ x_i^{t+1}, & \text{if } f(pbest_i^t) > f(x_i^{t+1}). \end{cases} \tag{38}$$

Finally, the global best of the swarm is updated using the following equation:

$$gbest^{t+1} = \text{argmin} \cdot f(pbest_i^{t+1}), \tag{39}$$

where f is a function that evaluates the fitness value for a given position.

The PSO process is repeated iteratively until one of the following termination criteria occurs [21] if the

maximum number of iterations has been reached, an acceptable solution should be found, or no improvement is observed over a number of iterations.

The PSO control parameters used in this study are; the population size is 60, maximum generation 100, the acceleration factors ($c_1 = 0.5$ and $c_2 = 1.25$) and the inertia weight ($w = 0.6$). It is noteworthy to mention that all the developed programs are under the commercial software Matlab-Simulink.

4. Application

4.1. Simulation of the System Behaviour

The simulation of the system behaviour reveals an important problem in the control. When the training speed is variable, the voltages and the currents of the exciter and the main generator vary in order to maintain the voltage at nominal value.

The problems mentioned before can be presented as follows:

In the case, where the training speed is high, the theoretical excitation voltage of the exciter and main generator that provides a nominal voltage (the voltage of the main generator) is low, due to the excitation voltage that is inversely proportional to the training speed. The difference between the voltage delivered by the PMG machine and the theoretical excitation voltage of the main generator and exciter is very important, which makes the control system, in this case, very complicated.

In the case of low speed, the voltage delivered by PMG machine can be insufficient to excite the main generator exciter group, because the excitation field of the PMG machine is constant.

Choosing PMG machine depends on specifications, i.e. expertise, knowledge and field of use. To overcome this problem (the insufficiency of PMG machine), the PMG machine with low speed (high number of poles) is used. This produces enough voltage to excite the group main generator-exciter. In order to control the output voltage of the BESG, the excitation voltage of the main exciter-generator group is calculated from the load and the speed.

The excitation voltage value corresponds to the rated voltage (220 V) which is considered as a reference of the voltage regulator of the MSAP (Fig. 5). At every moment and for a given speed, the excitation voltages of the main exciter and generator are calculated. Which will be a reference for the regulator voltage of the PMG, i.e. decrease the difference between the voltage delivered by PMG machine and excitation voltage of the main generator-exciter group. This ensures stability when the machine works at high speed. For each variation in speed or load, our system adapts its self to these changes.

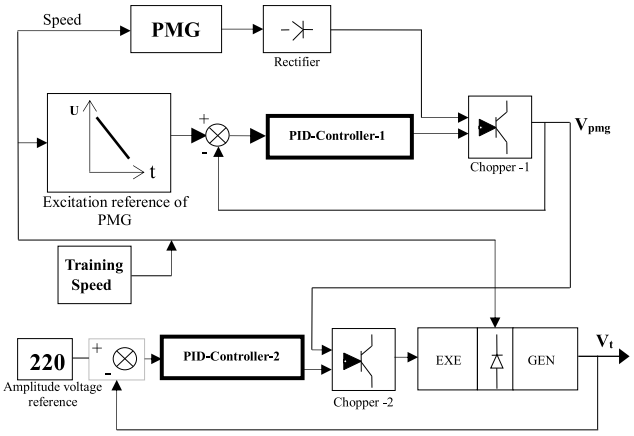

Fig. 5: Schematic diagram of brushless excitation synchronous generator control using PID-PSO controller.

4.2. Comparison Between PSO and Ziegler Nichols

In our case, Ziegler Nichols tuning is based on the open-loop step response of the system which is characterized by the following parameters; the process time constant L_z, the delay time and the time constant T_z.

These parameters are used to determine the controller's tuning parameters (see Tab. 1).

We note that the response of our system is a first order equation. The determination of controller parameters by the conventional methods such as Ziegler Nichols, for a given speed, is affordable. However, for the values of regulators parameters, that are adapted to the speed and load variations, are difficult to determine, and especially for the second controller, because the Ziegler Nichols method calculates the parameters of a single regulator (Fig. 5).

Thus, the parameters of the second controller are very difficult to be calculated, since it relies on the trial and error method as illustrate Fig. 5. The obtained simulation results for the PID controller using ZN method give the parameters:

$$K_{opt} = [K_{p1}, K_{i1}, K_{d1}, K_{p2}, K_{i2}, K_{d2}] = \\ = [2.08, 0.1664, 0.0486, 0.12, 1.22, 3.04]. \quad (40)$$

The parameters K_{p1}, K_{il} and K_{d1} are determined by Ziegler Nichols method (Tab. 1) while K_{p2}, K_{i2} and K_{d2} are determined by trial and error.

The simulation results are illustrated in Fig. 6. They reveal the behaviour of the voltage V_t of the main gen-

erator for an inductive load of $\cos(\varphi) = 0.8$. The response time of the main generator becomes faster and takes less than 0.2 s, and its operation is stable as shown in the zoom of Fig. 6.

In Fig. 6, the disruptions in high-speed region are due to incorrect values of the second regulator parameters. The determination of the parameters for several regulators using PSO technique is very useful.

Tab. 1: Ziegler-Nichols for open-loop tuning parameters.

Controller	K_{p1}	$T_{i1} = \frac{K_{p1}}{K_{i1}}$	$T_{d1} = \frac{K_{d1}}{K_p}$
P	$\frac{T_z}{L_z}$	-	0
PI	$0.9(\frac{T_z}{L_z})$	$\frac{L_z}{0.3}$	0
PID	$1.2(\frac{T_z}{L_z})$	$2L_z$	$0.5L_z$

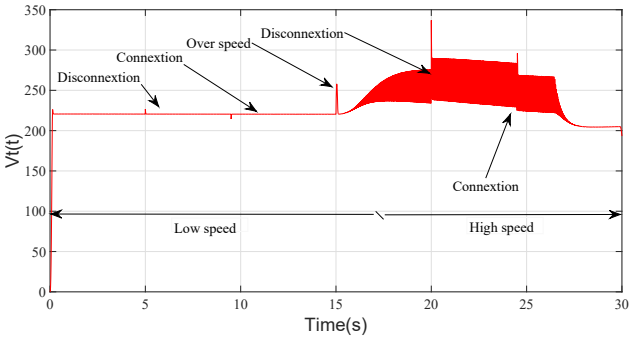

Fig. 6: Variation of the main generator voltage for inductive load: $\cos(\varphi) = 0.8$ using Ziegler Nichols method.

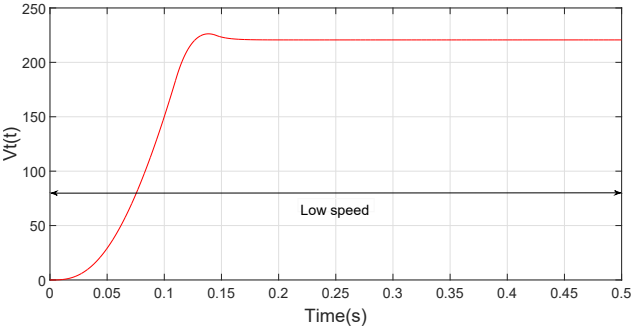

Fig. 7: Zoom of Fig. 6 between 0 and 0.5 s.

The PSO method is used to optimize the parameters of the regulators off-line, however, in on-line control, the regulator parameters must be calculated by PSO, when the speed vary.

4.3. Simulation Results and Discussion

In order to optimize the parameters of the PID controller, the PSO is implemented in Matlab-Simulink environment. The results obtained when the main generator running at full load with a power of 7 kVA.

The simulation results are illustrated in Fig. 8. They illustrate the behaviour of the voltage V_t of the main generator of an inductive load of $\cos(\varphi) = 0.8$.

When the training speed reaches 314 rad·s^{-1} for inductive load ($\cos(\varphi) = 0.8$), the response time of the main generator becomes faster and takes less than 0.2 s, and its operation is stable as shown in zoom of Fig. 8(a). When a load is applied at the terminals of the main generator, the voltage amplitude follows the reference in both cases corresponding to the connection and the disconnection of the rated load, as shown in zoom of figure Fig. 8(b). One can note that the effect of the load variation is perfectly damped, and the system, in this case, rejects all disturbances.

In the same configuration, when the training speed reaches 3140 rad·s^{-1}, a voltage peak at the 15$^{\text{th}}$ second is observed. When speed varies from 314 rad·s^{-1} to 3140 rad·s^{-1}, as illustrated in the zoom of Fig. 8(c), the peak duration is less than 0.2 s and the voltage is stable and has amplitude less than 20 % of the nominal one.

At high speed of 3140 rad·s^{-1}, illustrated in the zoom of Fig. 8(c), when a load is applied at the terminals of the main generator. In these cases of connection and disconnection, the voltage amplitude follows the reference and the variation effect of the load is perfectly damped, Fig. 9. In high-speed case, the amplitude of the voltage peak, at 20$^{\text{th}}$ and 25$^{\text{th}}$ seconds, is more important but acceptable (in the norms; less than 20 %) and the stability time is also acceptable that justify the robustness of the control technique.

Table 2 shows the PSO parameters that are used for verifying the performance of the PSO-PID controller for searching the PID controller parameters. Inertia weight factor is set by:

$$\omega = \omega_{\max} - \left(\frac{(\omega_{\max} - \omega_{\min})}{iter_{\max}}\right) iter, \tag{41}$$

where $\omega_{\max} = 0.9$, $\omega_{\min} = 0.4$, $iter_{\max}$ is the maximum number of iterations, and iter is the current number of iterations. For these settings, the simulation result that shows the best solution corresponds to the PID parameters given:

$$K_{opt} = [K_{p1}, K_{i1}, K_{d1}, K_{p2}, K_{i2}, K_{d2}] = \\ = [99.96, 1.956, 2.407, 100, 0.201, 63.86]. \tag{42}$$

Tab. 2: The PSO parameters used in simulation.

Parameters	Value
α	10
β	4
Population size :n	50
c_1	2
c_2	2

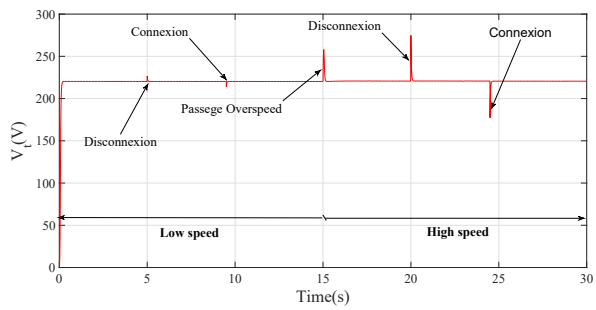

(a) V_t Voltage variation of the main generator with inductive load: $\cos(\varphi) = 0.8$.

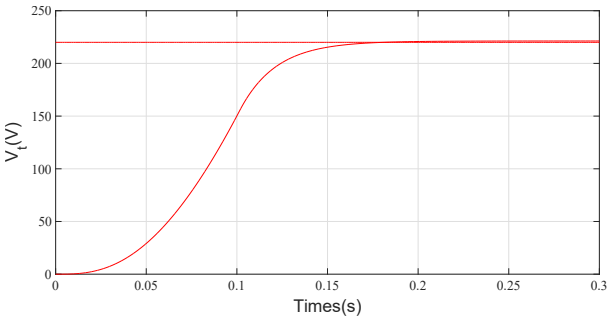

(b) Zoomed between 0 and 0.5 s.

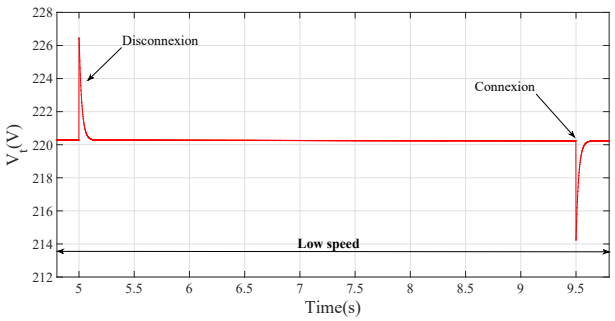

(c) Zoomed between 4.5 and 10 s.

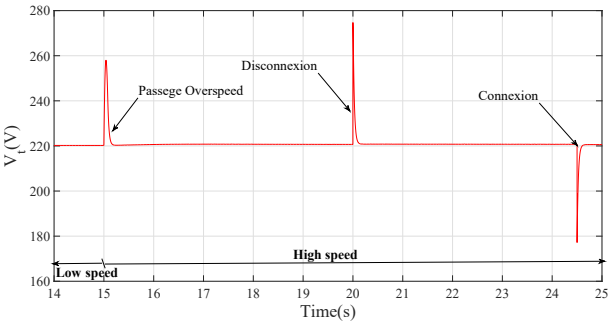

(d) Zoomed between 14 and 25 s.

Fig. 8: V_t Voltage variation of the main generator with inductive load: $\cos(\varphi) = 0.8$ with zoomed areas.

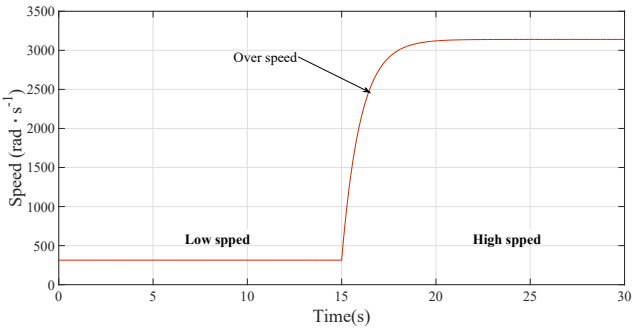

Fig. 9: Drive speed variation of brushless excitation synchronous generator.

4.4. Robustness Study

The robustness control is studded through parameters variation. It is justified when the machine operates at high speed due to the Foucault courant and the temperature effects which are considerable important.

In order to illustrate the robustness of the proposed control, the effect of the variation of main generator parameters on the performances of the voltage setting is studied.

The variation introduced in the test refers in practice to the real condition as overheating, saturation of the magnetic circuit and the operating conditions such as the variation of the speed and the load.

Three cases are considered:

- Variation in the stator resistance of 50 %.
- Variation in the rotor resistance of 50 %.
- Starting with low speed of 100 rad·s^{-1}.

To illustrate the performances of setting, the variation of stator and rotor resistance of 50 % compared to the rated values, with a voltage step of 220 V has been simulated. Figure 10 and Fig. 11 illustrate the test results which illustrate that the proposed technique is insensitive to the machine rotor or stator resistances variations. Hence, with even poorly determined parameters, the adopted control technique withstands and stays stable.

For the third simulated case, at a low speed (100 rad·s^{-1}) with application of a rated load, the system is always insensitive to this speed, as shown in Fig. 12. The control system ensures the disturbances rejection in three cases considered (the time constants of the system are greater than those of the machine). The proposed control technique presented in this paper is robust, simple and has the advantage of being easily implemented.

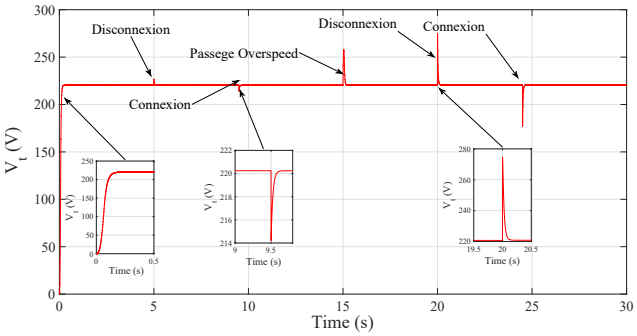

Fig. 10: Robustness test for the stator resistance R_s variation (50 % increase of the stator resistance).

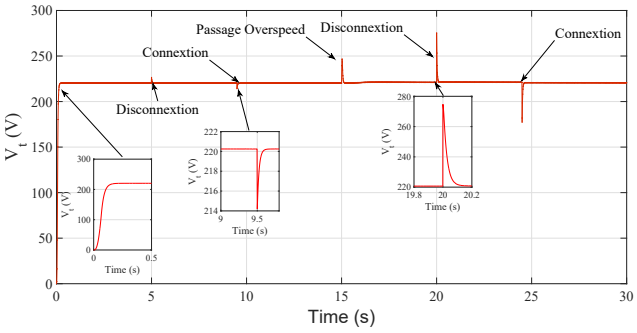

Fig. 11: Robustness test for the rotor resistance R_r variation (50 % increase of the rotor resistance).

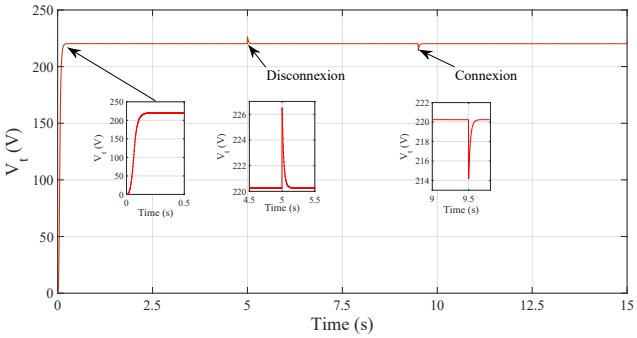

Fig. 12: Robustness test for the Starting with low speed of 100 rad·s^{-1}.

5. Conclusion

To resolve the problem of brushless synchronous generator machine control, a new strategy is proposed. A simulation of direct current machine is used, which allows to understand well the difficulties of the control. For this, an optimization of the voltage amplitude control of the BESG by using PSO has been realized.

The results show that by the control of the voltage excitation of the exciter, which is the only physical parameter available, the voltage of the main generator is maintained at its reference value. This technique of control offers stability to the total voltage of the generator and rejects all disturbances regardless of the variation of the rotation speed or load.

The parameters optimization of the regulator using PSO is considered important for the control of complex systems, in our case the three-cascade synchronous machine. The result of the voltage amplitude control is considered good and better compared to the conventional control techniques.

References

[1] CARDENAS, R., J. CLARE and P. WHEELER. 4-Leg Matrix Converter Interface for a Variable-Speed Diesel Generation System. In: *38th Annual Conference on Industrial Electronics Society (IECON)*. Montreal: IEEE, 2012, pp. 6044–6049. ISBN 978-1-46732-420-5. DOI: 10.1109/IECON.2012.6389093.

[2] WANG, D. H., C. V. NAYAR and C. WANG. Modeling of Stand-alone Variable Speed Diesel Generator using Doubly-Fed Induction Generator. In: *2nd International Symposium on Power Electronics for Distributed Generation Systems (PEDG)*. Hefei: IEEE, 2010, pp. 1–6. ISBN 978-0-470-64337-2. DOI: 10.1109/PEDG.2010.5545769.

[3] NASR, A., S. HLIOUI, M. GABSI, M. MAIRIE and D. LALEVEE. Experimental investigation of a Doubly-Excited Flux-Switching Machine for Aircraft DC Power Generation. In: *International Electric Machines and Drives Conference (IEMDC)*. Miami: IEEE, pp. 1–7. ISBN 978-1-5090-4281-4. DOI: 10.1109/IEMDC.2017.8002113.

[4] PATIN, N., L. VIDO, E. MONMASSON, J. P. LOUIS, M. GABSI and M. LECRIVAIN. Control of a Hybrid Excitation Synchronous Generator for Aircraft Applications. *IEEE Transaction on Industrial Electronics.* 2008, vol. 55, iss. 10, pp. 3772–3783. ISSN 0278-0046. DOI: 10.1109/TIE.2008.924030.

[5] BAYRAM, T. and A. STEPHAN. Comparative Study of Power Electronics Converters Associated to Variable Speed Permanent Magnet Alternator. In: *International Symposium on Power Electronics Electrical Drives, Automation and Motion (SPEEDAM)*. Taormina: IEEE, 2006, pp. 1332–1337. ISBN 1-4244-0193-3. DOI: 10.1109/SPEEDAM.2006.1649974.

[6] KRAVTZOFF, I., P. DESSANTE, J. C. VANNIER, P. MANFE and E. MOUNI. Global Optimization of Hybrid Electrical System to Decrease Fuel Consumption or Operating Cost. In: *Power Electronics and Applications European Conference.* Lappeenranta: IEEE, 2014, pp. 1–8. ISBN 978-1-4799-3016-6. DOI: 10.1109/EPE.2014.6910875.

[7] KRAVTZOFF, I., P. DESSANTE, J. C. VANNIER, P. MANFE and E. MOUNI. Optimal Control Strategy to Design a Hybrid Electrical System. In: *Power Electronics Machines and Drives International Conference.* Manchester: IET, 2014, pp. 1–6. ISBN 978-1-84919-815-8. DOI: 10.1049/cp.2014.0409.

[8] ROSADO, S., X. MA, G. FRANCIS, F. WANG and D. BOROYEVICH. Model-Based Digital Generator Control Unit for a Variable Frequency Synchronous Generator with Brushless Exciter. *IEEE Transactions on Energy Conversion.* 2008, vol. 23, iss. 1, pp. 42–52. ISSN 0885-8969. DOI: 10.1109/TEC.2006.888040.

[9] MAALOUF, A., M. W. NAOUAR, E. MONMASSON, A. A. NAASSANI, S. LEBALLOIS and J. MIDY. Digital Control of Brushless Excitation Synchronous Starter/Generator in the Generation Mode. In: *34th Annual Conference on Industrial Electronics Society (IECON).* Orlando: IEEE, 2008, pp. 1155–1160. ISBN 978-1-4244-1767-4. DOI: 10.1109/IECON.2008.4758117.

[10] SHABIB, G., A. G. MOSLEM and A. M. RASHWAN. Optimal Tuning of PID Controller for AVR System Using Modified Particle Swarm Optimization. In: *International Conference on Fuzzy Systems.* Barcelona: IEEE, 2005, pp. 104–110. ISBN 978-960-474-195-3.

[11] GAING, Z. L. A Particle Swarm Optimization Approach for Optimum Design of PID Controller in AVR System. *IEEE Transactions on Energy Conversion.* 2004, vol. 19, iss. 2, pp. 384–391. ISSN 0885-8969. DOI: 10.1109/TEC.2003.821821.

[12] AMER, M. L., H. H. HASSAN and H. M. YOUSSEF. Modified Evolutionary Particle Swarm Optimization for AVR-PID Tuning. In: *Communications and Information Technology, Systems and Signals.* Attica: IEEE, 2008, pp. 164–173. ISBN 978-960-6766-69-5.

[13] LI, W., X. ZHANG and H. LI. Novel Digital Automatic Voltage Regulator for Synchronous Generator. In: *International Conference on Power System Technology (POWERCON).* Zhejiang: IEEE, 2010, pp. 1–6. ISBN 978-1-4244-5938-4. DOI: 10.1109/POWERCON.2010.5666631.

[14] WEILIN, L., Y. YANG and X. ZHANG. Digital Generator Control Unit Design for a Variable Frequency Synchronous Generator in MEA. *Energies.* 2018, vol. 11, iss. 1, pp. 1–17. ISSN 1996-1073. DOI: 10.3390/en11010096.

[15] MUKHERJEE, V. and S. P. GHOSHAL. Intelligent Particle Swarm Optimized Fuzzy PID Controller for AVR System. *Electric Power Systems Research.* 2007, vol. 77, iss. 12, pp. 1689–1698. ISSN 0378-7796. DOI: 10.1016/j.epsr.2006.12.004.

[16] KENNEDY, J. and R. C. EBERHART. Particle Swarm Optimization. In: *International Conference on Neural Networks.* Perth: IEEE, 1995, pp. 1942–1948. ISBN 0-7803-2768-3. DOI: 10.1109/ICNN.1995.488968.

[17] RAJENDRA, R. and D. K. PRATIHAR. Particle Swarm Optimization Algorithm vs Genetic Algorithm to Develop Integrated Scheme for Obtaining Optimal Mechanical Structure and Adaptive Controller of a Robot. *Intelligent Control and Automation.* 2011, vol. 2, iss. 4, pp. 430–449. ISSN 2153-0653. DOI: 10.4236/ica.2011.24050.

[18] EL-ABD, M. *Cooperative Models of Particle Swarm Optimizers.* Waterloo, 2008. Dissertation thesis. University of Waterloo. Supervisor prof. Mohamed Kamel.

[19] ROBINSON, J. and Y. RAHMAT-SAMII. Particle Swarm Optimization in Electromagnetics. *IEEE Transactions on Antennas and Propagation.* 2004, vol. 52, iss. 2, pp. 397–407. ISSN 0018-926X. DOI: 10.1109/TAP.2004.823969.

[20] NABAVI-KERIZI, S. H., M. ABADI and E. KABIR. A PSO-based Weighting Method for Linear Combination of Neural Networks. *Computers and Electrical Engineering.* 2010, vol. 36, iss. 5, pp. 886–894. ISSN 0045-7906. DOI: 10.1016/j.compeleceng.2008.04.006.

[21] BEDI, P., R. BANSAL and P. SEHGAL. Using PSO in a Spatial Domain based Image Hiding Scheme with Distortion Tolerance. *Computers and Electrical Engineering.* 2013, vol. 39, iss. 2, pp. 640–654. ISSN 0045-7906. DOI: 10.1016/j.compeleceng.2012.12.021.

About Authors

Hassen SMAIL was born in Batna, Algeria, in 1965. He receives the B.Sc. degree in electrical engineering from the University of Batna, Algeria, in 1990, and the M.Sc. degree in electrical networks from the Electrical Engineering Institute of Batna University, Algeria, in 1996. Currently, he is a Teaching Assistant at the University of Batna. His major fields of interest in research are diagnosis, identification and control of electrical machines.

Mostafa Kamel SMAIL is an associate professor in the Aerospace Systems department of Polytechnic Institute of Advanced Science-Paris-France. He received the master degree in components and antennas for

telecommunications in 2007 and the Ph.D. degree from University of Paris-Sud XI, France in 2010. His current research interests are wave propagation modeling, reliability of wiring, electromagnetic compatibility and Inverse modeling.

Cherif FETHA was born in Batna, Algeria, in 1958. He receives the B.Sc. degree in electrical engineering from Badji Mokhtar University of Annaba, and the M.Sc. degree in Electrical networks from the Electrical Engineering Institute of Batna University, Algeria, in 1993. He receives the Ph.D. degree in Electrical networks from the University of Batna Algeria where he is currently a Professor of electrical engineering with the Electrical Engineering Institute at the University of Batna. His major fields of interest in research are diagnosis, Electrical networks and control of electrical machines.

Tahar BAHI received the Engineer, Magister and Doctorat degrees in electrical engineering from Badji Mokhtar University, Annaba, Algeria in 1983, 1986 and 2006 respectively. Since 1983, he has been with the Department of Electrical of the University of Annaba, Annaba, Algeria where he is currently a Professor of electrical engineering. His main research fields include electrical machines, power electronics and drive, diagnosis and fault tolerant control and renewable energy applications.

Appendix

Main synchronous machine parameters 7 kVA, 220 V, $U_{\mathrm{f}} = 10$ V, 50 Hz, 3 phases, Y connection, 2 poles.

Tab. 3: Dimension of the main synchronous machine parameters.

Stator resistance	$R_s = 0.01\ \Omega$
D axis stator inductance	$L_D = 0.002985$ H
Q axis stator inductance	$L_Q = 0.001487$ H
Rotor resistance	$R_F = 0.32165\ \Omega$
Mutual inductance	$MAF = 0.02889$ H
Rotor stator inductance	$L_F = 0.03088$ H